

Classical versus quantum dynamics for a driven relativistic oscillator

R. E. Wagner, P. J. Peverly, Q. Su, and R. Grobe

Intense Laser Physics Theory Unit and Department of Physics, Illinois State University, Normal, Illinois 61790-4560

(Received 17 September 1999; published 17 February 2000)

We compare the time evolution of the quantum-mechanical spatial probability density obtained by solving the time-dependent Dirac equation with its classical counterpart obtained from the relativistic Liouville equation for the phase-space density in a regime in which the dynamics is essentially relativistic. For a resonantly driven one-dimensional harmonic oscillator, the simplest nontrivial model system to perform this comparison, we find that, despite the nonlinearity induced by relativity, the classical ensemble description matches the quantum evolution remarkably well.

PACS number(s): 32.80.-t, 03.65.-w

It is well known that for linear systems the time evolution of quantum-mechanical observables can also be described by the corresponding average values obtained from the classical phase-space density [1]. The Heisenberg equations of motion for the quantum operators and their corresponding expectation values in this special case are formally identical to the corresponding dynamical equations for the classical average values.

In the more interesting general case of a nonlinear system, however, the correspondence between the exact quantum description and the classical description using phase-space densities is not so clear. For instance, if the quantum-mechanical Wigner function obtained from the quantum state is negative, it is believed that the corresponding classical description could be inappropriate. In the case of nonchaotic dynamics, several case studies have suggested that the quantum and classical ensemble average values are very similar on a time scale inversely proportional to Planck's constant representing the effective action. In the case of a bound quantum system, the system does not realize the discreteness of the underlying energy levels and the dynamics is basically classical until the characteristic quantum recurrences occur [2,3]. For classically chaotic dynamics the time scales for which the two approaches agree is much shorter, and only proportional to the logarithm of Planck's constant [4,5]. In almost all studies that investigated the classical and quantum-mechanical correspondence, the nonlinearity of the dynamics was due to either the time-independent or time-dependent interaction force. In this work, we investigate the nonlinearity induced by the velocity in the high-speed, relativistic regime.

The new dynamical features that relativity can bring to the time evolution for a classical system have recently been demonstrated by Kim and Lee [6]. They showed that in contrast to the trivial and fully analytically soluble dynamics [1] of the driven harmonic oscillator, the relativistic case exhibits resonance overlap and chaos that normally is associated with driven nonlinear oscillators. They suggested that relativistic chaos requires at least a quadratic potential, while nonrelativistic chaos needs at least a cubic term in the potential. In a related work, [7] chaotic signatures such as nonlinear resonances, stochastic layers near resonance separatrices, bifurcations of fixed points, and reconnection phenomena have also been associated with the relativistic cyclotron motion of electrons.

The exploration of the relativistic quantum dynamics relies in general on the wave-function solution of the time-dependent Dirac equation. These solutions are very difficult to obtain analytically; for a few exceptions see Ref. [8]. To overcome this technical limitation and to obtain some first insights into the relativistic dynamics, numerical solution techniques are required. This computational challenge has been taken in the study of relativistic heavy ion collisions [9–11], and was recently performed to simulate the interaction of atoms in intense laser fields [12–15]. However, the limitations due to the finite CPU time and memory, even on the fastest supercomputers, are quite severe, and restrict the accessible parameter regime that can be studied. For the case of the relativistic atom-laser interaction, for which effects due to the generation of antiparticles are not so important (yet), a first insight into the dynamics can be obtained by inspecting the corresponding classical, but relativistic, dynamics of the phase-space density [16–18]. For these case studies it is quite crucial to determine whether classical predictions can be trusted even qualitatively in regimes for which the nonlinearity induced by the high-speed motion of the electrons is the dominant factor for the evolution.

The simplest system for which no analytical solution exists, and for which the impact of relativity on the classical and quantum-mechanical system can be compared, is the one-dimensional harmonic oscillator with the potential $V(x) = \omega_0^2 x^2/2$ driven by a time-dependent periodic force of strength E and frequency ω_L . Classically, its time evolution generator is described by the Hamilton function H_{cl} in atomic units:

$$H_{cl} = \sqrt{c^4 + c^2[p - E/\omega_L \sin(\omega_L t)]^2} + V(x). \quad (1)$$

We should note that the relativistic dynamics can be solved exactly only for two simpler cases, $V(x) = 0$ (free particle) and $V(x) \approx x$ (free-fall), for which the classical and quantum-mechanical solutions can be expressed analytically and agree [1]. The classical spatial probability density $P_{cl}(x, t)$ can be obtained from the phase-space density $\rho(x, p, t)$ via $P_{cl}(x, t) \equiv \int dp \rho(x, p, t)$, which is a solution of the relativistic Liouville equation [19]

$$\begin{aligned} \partial \rho(x, p, t) / \partial t = & (\partial H_{cl} / \partial x) \partial \rho(x, p, t) / \partial p \\ & - (\partial H_{cl} / \partial p) \partial \rho(x, p, t) / \partial x. \end{aligned} \quad (2)$$

We should stress that the simplicity of the model was chosen for convenience only; our interest here is clearly not to simulate a specific physical system in every detail, but to investigate a prototype model system that includes just the minimum ingredients to be useful as a working model to compare the classical and quantum-mechanical predictions. However, we might also note that the dynamics of an electron in a uniform static magnetic field interacting with a resonant laser field [7,17,18] is similar to the dynamics investigated here. The latter suggests that the (standing-wave) dipole approximation and the space-dimensional restriction used here are not crucial at all to discuss the basic physics. Also, we neglect radiative corrections that could affect the motion for extreme-ultrarelativistic speeds for a charged particle.

The corresponding relativistic quantum mechanical spatial probability density is $P_{\text{qm}}(x,t) = \sum_{i=1}^4 |\Psi_i(x,t)|^2$, where the summation extends over the four spinor components. It can be obtained from the corresponding numerical wave function solution to the Dirac equation (in atomic units):

$$i\partial\Psi/\partial t = -ic\alpha_x\partial\Psi/\partial x + \alpha_x A\Psi + c^2\beta\Psi + V(x)\Psi. \quad (3)$$

Here α_x and β denote the 4×4 Dirac matrices, and $A = -cE/\omega_L \sin(\omega_L t)$. The time-dependent solution of the wave function $\Psi(x,t) = \{\Psi_1, \Psi_2, \Psi_3, \Psi_4\}$ can be obtained on a space-time grid using a split-operator algorithm based on fast Fourier transformation that is accurate up to the fifth order in time [15]. In all of our simulations presented below, the spatial axis was discretized into 16 384 grid points, which together with up to 1 500 000 temporal points led to fully converged results. The classical Liouville equation was solved via a Monte Carlo technique in which the phase-space density was discretized along 10 000 appropriately weighted classical relativistic orbits.

For simplicity, as an initial state we use the ground state of the harmonic oscillator $\Psi_1(x,t=0) = (\omega_0/\pi)^{1/4} \exp(-\frac{1}{2}\omega_0 x^2)$, where for convenience we have set the remaining three spinor components to zero. The corresponding classical probability distribution was (arbitrarily) chosen to be factorized $\rho(x,p,t=0) = 1/\pi \exp[-\omega_0 x^2] \exp[-p^2/\omega_0]$ for which all average values $\langle x^n p^m \rangle_{\text{cl}} \equiv \iint dx dp x^n p^m \rho(x,p,t=0)$ match the initial (symmetrized) quantum-mechanical expectation values $[\langle x^n p^m \rangle_{\text{qm}} + \langle p^m x^n \rangle_{\text{qm}}]/2$ for all positive integers n and m .

In Fig. 1(a) we show three snapshots of the exact quantum-mechanical spatial probability density $P_{\text{qm}}(x,t)$ after zero, four, and eight cycles of the external force. Superimposed are the predictions from the corresponding classical space density $P_{\text{cl}}(x,t)$. The graphs are practically indistinguishable.

This agreement is quite remarkable because the dynamics is basically relativistic. The corresponding nonrelativistic solution displayed in Fig. 1(b) is quite different. The distribution according to nonrelativistic Schrödinger [20,21] and classical Liouville theory match, and can be found analytically:

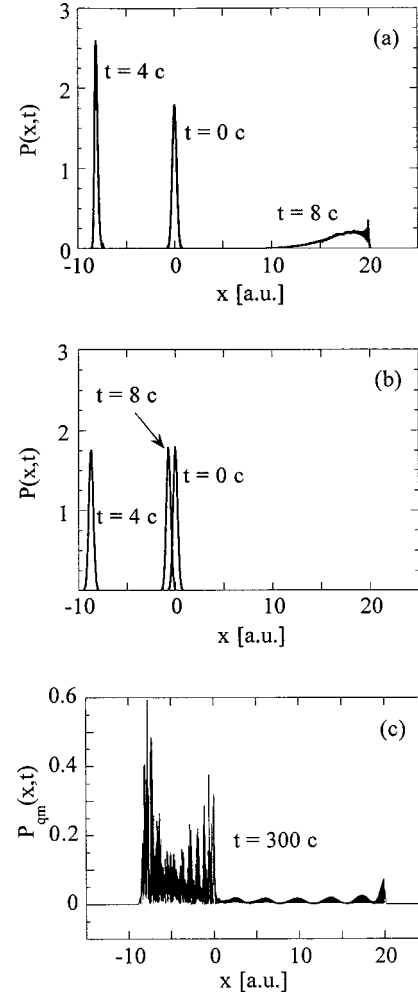


FIG. 1. Comparison of the relativistic and nonrelativistic spatial probability densities calculated from the Dirac equation, the Schrödinger equation, and the classical Liouville equation. The temporal snapshots were taken at times $t=0, 4,$ and 8 cycles of the external driving force. (a) Solution of the time-dependent Dirac equation, $P_{\text{qm}}(x,t)$. Superimposed on each of the three graphs is the solution of the relativistic Liouville equation, $P_{\text{cl}}(x,t) = \int dp \rho(x,p,t)$. (b) Solution of the time-dependent Schrödinger equation, $P_{\text{qm}}(x,t) = |\Psi(x,t)|^2$. Superimposed on each graph is the solution of the non-relativistic Liouville equation, $P_{\text{cl}}(x,t) = \int dp \rho(x,p,t)$. (c) The Dirac equation prediction for the spatial distribution after 300 cycles. The parameters were $E=100$ a.u., $\omega_0=10$ a.u., and $\omega_L=8.8$ a.u.

$$P_{\text{cl}}(x,t) = P_{\text{qm}}(x,t) = \left(\frac{1}{2\pi\Delta x^2(t)} \right)^{1/2} \exp\left[-(x - \xi(t))^2 / (2\Delta x^2(t)) \right] \quad (4)$$

where the time-dependent parameter $\xi(t) = -E[\cos(\omega_L t) - \cos(\omega_0 t)]/(\omega_0^2 - \omega_L^2)$ denotes the motion of the center of the distribution, and $\Delta x^2(t) = \Delta x^2 \cos^2(\omega_0 t) + \sin^2(\omega_0 t)/(4\omega_0^2 \Delta x^2)$ its time-dependent spatial variance.

In Fig. 1(c) we show the relativistic distribution after 300 cycles. Several features characterize the quantum distribution. It is highly oscillatory in space, and the wave packet

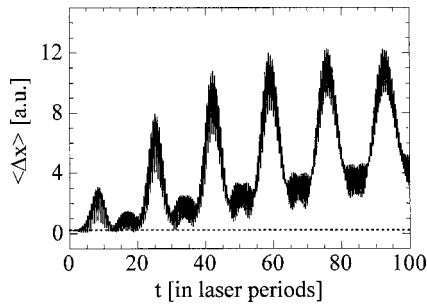


FIG. 2. Time evolution of the spatial width of the distribution $\langle \Delta x \rangle$ according to the Dirac equation and the relativistic Liouville equation. The two curves are practically indistinguishable. The (constant) dashed line corresponds to the (analytical) prediction of the (nonrelativistic) Schrödinger equation, which matches the curve from the nonrelativistic Liouville equation.

seems to consist of two different types of relativistic structures. A more irregular part for $-8 \text{ a.u.} < x < 0$ and a periodic part for $0 < x < 20 \text{ a.u.}$ Most importantly, we have noticed an extreme degree of localization. The wave packet falls off by more than 30 orders of magnitude within less than 1 a.u. A repeated simulation for smaller spatial and temporal grid-points clearly confirm that this extreme degree of sharp localization is not a numerical artifact. In addition, the corresponding classical ensemble solution also shows this quite unexpected localization. Clearly more detailed investigations of this relativistic effect are in order.

A comparison between the quantum-mechanical expectation value of the position $\langle x \rangle$ and the ensemble-averaged position $\langle x \rangle_{cl}(t)$ do not reveal any major difference in the rela-

tivistic domain. In Fig. 2 we view the same process via the time evolution of the spatial widths $\langle \Delta x \rangle_{qm}(t)$ and $\langle \Delta x \rangle_{cl}(t)$. Again, the nonrelativistic curve can be easily obtained analytically. For our initial width of $\Delta x = 1/\sqrt{[2\omega_0]}$ it becomes time independent: $\langle \Delta x \rangle_{qm} = \langle \Delta x \rangle_{cl} = \Delta x$, which is shown by the dashed line.

The relativistic solutions, however, show a quite distinct behavior. The widths increase in an oscillatory fashion to a maximum value close to 12 a.u. The growth pattern is characterized by a short-time scale of the half-laser cycle, and a longer one with a period of about 18 laser cycles. After about 300 laser cycles (not shown) the widths reach an almost steady value [22]. We should point out that the quantum and classical predictions are practically indistinguishable. The nonrelativistic width does not depend on the driving strength E ; however, the relativistic solution does.

To summarize, in this Brief Report we have demonstrated that, for a simple model system, the approximation of relativistic quantum dynamics by a classical phase-space density can be quite reasonable even in the high-speed regime in which the nonlinearity induced by relativity determines almost all aspects of the evolution, and the classical dynamics can reveal chaotic behavior.

We acknowledge helpful conversations with M. V. Fedorov, C. C. Gerry, P. Krekora, R. F. Martin, and H. Wanare. This work was supported by the NSF under Grant No. PHY-9970490. We also acknowledge support from the Research Corporation for Cottrell Science Awards and ISU for URGs. R.E.W. and P.J.P. thank the Illinois State University Undergraduate Honors Program for support of their research work. The numerical work was performed at NCSA.

-
- [1] H. C. Kim, M. H. Lee, J. Y. Ji, and J. K. Kim, Phys. Rev. A **53**, 3767 (1996), and references therein.
 - [2] K. Bhattacharyya and D. Mukhrtjee, J. Chem. Phys. **84**, 3212 (1986).
 - [3] T. Hogg and B. A. Huberman, Phys. Rev. Lett. **48**, 711 (1982).
 - [4] F. Haake, *Quantum Signatures of Classical Chaos* (Springer-Verlag, Berlin, 1991).
 - [5] F. Haake, M. Kus, and R. Scharf, Z. Phys. B: Condens. Matter **65**, 381 (1987).
 - [6] J. H. Kim and H. W. Lee, Phys. Rev. E **51**, 1579 (1995); **52**, 473 (1995); S. W. Lee, J. H. Kim, and H. W. Lee, *ibid.* **56**, 4090 (1997).
 - [7] J. H. Kim and H. W. Lee, Phys. Rev. E **54**, 3461 (1996).
 - [8] For a collection of the few analytically soluble cases, see V. G. Bagrov and D. M. Gitman, *Exact Solutions of Relativistic Wave Equations* (Kluwer, Dordrecht, 1990).
 - [9] C. Bottcher and M. R. Strayer, Ann. Phys. (N.Y.) **175**, 64 (1987).
 - [10] J. C. Wells, A. S. Umar, V. E. Oberacker, C. Bottcher, M. R. Strayer, J.-S. Wu, J. Drake, and R. Flanery, Int. J. Mod. Phys. C **4**, 459 (1993).
 - [11] K. Momberger, A. Belkacem, and A. H. Sorensen, Phys. Rev. A **53**, 1605 (1996).
 - [12] U. W. Rathe, C. H. Keitel, M. Protopapas, and P. L. Knight, J. Phys. B **30**, L531 (1997).
 - [13] N. J. Kylstra, A. M. Ermolaev, and C. J. Joachain, J. Phys. B **30**, L449 (1997).
 - [14] C. Szymanowski, C. H. Keitel, and A. Maquet, Laser Phys. **9**, 133 (1999).
 - [15] J. W. Braun, Q. Su, and R. Grobe, Phys. Rev. A **59**, 604 (1999).
 - [16] C. H. Keitel, P. L. Knight, and K. Burnett, Europhys. Lett. **24**, 539 (1993); C. H. Keitel and P. L. Knight, Phys. Rev. A **51**, 1420 (1995).
 - [17] R. E. Wagner, Q. Su, and R. Grobe, Bull. Am. Phys. Soc. **44**, 634 (1999); Phys. Rev. A **60**, 3233 (1999).
 - [18] R. E. Wagner, Q. Su, and R. Grobe (unpublished).
 - [19] H. Goldstein, *Classical Mechanics*, 2nd ed. (Addison-Wesley, New York, 1980).
 - [20] For a discussion on the nonrelativistic limit, see B. Thaller, *The Dirac Equation* (Springer, Berlin, 1992), Chap. 6.
 - [21] The nondriven time evolution is described in L. I. Schiff, *Quantum Mechanics*, 3rd ed. (McGraw-Hill, New York, 1968).
 - [22] For relativistic suppression of spatial spreading, see Q. Su, B. A. Smetanko, and R. Grobe, Opt. Express **2**, 277 (1998); Laser Phys. **8**, 93 (1998).